

# NEUTRON SCATTERING SHOWS THAT CYTOCHROME $b_5$ PENETRATES DEEPLY INTO THE LIPID BILAYER

E. P. GOGOL AND D. M. ENGELMAN

*Department of Molecular Biophysics and Biochemistry, Yale University, New Haven, Connecticut 06511*

**ABSTRACT** Cytochrome  $b_5$  was asymmetrically reconstituted into small lipid vesicles made of a highly deuterated phospholipid. Small-angle neutron diffraction patterns were collected in a series of  $H_2O$ - $D_2O$  mixtures from vesicles consisting of lipid and native or trypsinized cytochrome  $b_5$ . The second moment of the radial distribution of scattering density in the vesicles was derived from these data and was compared to values calculated from three proposed models, which differ by the degree that cytochrome  $b_5$  penetrates the lipid bilayer. The model in which the hydrophobic domain of the protein is distributed across the bilayer agreed most closely with the data.

## INTRODUCTION

Cytochrome  $b_5$  is an anchored membrane protein comprised of two domains: a hydrophilic catalytic portion, which is structurally well characterized (e.g., Mathews et al., 1970), and a hydrophobic membrane-binding segment (Spatz and Strittmatter, 1971). Physical and chemical studies (Fleming et al., 1979; Dailey and Strittmatter, 1981) have elucidated various aspects of the interaction of the membrane-binding segment with lipid bilayers, but have not addressed the question of its time-averaged mass distribution. Diffraction methods, or scattering from randomly oriented particles in solution, can yield information on the overall structure of the protein. Previous solution-scattering studies of membrane proteins (e.g., Yeager, 1975; Osborne et al., 1978) have been performed in the presence of detergents, where it is assumed that the protein structure is preserved, and where interactions with lipid are revealed only by implication. In this study, we examined the structure of cytochrome  $b_5$  bound to lipid vesicles using neutron small-angle scattering methods. To increase scattering contrast between lipid and protein, a highly deuterated phospholipid was prepared and used to reconstitute cytochrome  $b_5$  into vesicles. A range of low-resolution models was considered to explain the arrangement of the protein with respect to the vesicle membrane. The scattering properties of the models were calculated, and the results were compared with experimentally observed parameters to evaluate the models.

## METHODS

Using an established protocol (Strittmatter et al., 1978), cytochrome  $b_5$  was isolated from fresh steer liver by Dr. Phillip Strittmatter and stored frozen until used. A highly deuterated phosphatidylcholine (PC) was

prepared from *E. coli* lipids and analyzed as previously reported (Gogol et al., 1983). The preparation and analysis of sonicated lipid vesicles and the asymmetric incorporation of cytochrome  $b_5$  into them (cytochrome  $b_5$  vesicles) has also been described (Gogol et al., 1983). Protein concentrations in these samples were measured spectroscopically (Spatz and Strittmatter, 1971), and lipid concentrations were determined by phosphate assay (Bartlett, 1959).

In addition to the native cytochrome  $b_5$  vesicles, cytochrome  $b_5$  vesicles depleted of the protein's catalytic domain (trypsinized vesicles) were prepared by proteolysis and column chromatography. 4 mg of trypsin (Sigma Chemical Co., St. Louis MO) was dissolved in 0.2 ml vesicle buffer (20 mM Tris-acetate with 0.2 mM EDTA and 0.02%  $NaNO_3$ ) pH 8.1 and added to 1 ml of cytochrome  $b_5$  vesicles (5 mmol PC, 0.25 mmol cytochrome  $b_5$ ) in buffer containing 0.5 M NaCl. The mixture was incubated overnight at 4 °C and applied to a  $0.5 \times 20$  cm Sephadex G-100 column (Pharmacia Fine Chemicals, Piscataway NJ), which had been pre-run with deuterated PC vesicles. Fractions obtained at the void volume were pooled, analyzed, and used for diffraction experiments within 24 h. Spectroscopic analysis indicated that 80% of the heme domain was removed from the sample, which agrees with previous trypsin treatments.

Samples used for neutron-scattering experiments (lipid vesicles, cytochrome  $b_5$  vesicles, and trypsinized vesicles) were dialyzed overnight against vesicle buffer (including 0.2 or 0.5 M NaCl) made with  $H_2O$  or  $D_2O$ , and mixed to obtain the desired intermediate solvent composition. Small-angle, neutron-scattering patterns were recorded on the multidetector on instrument D11 at the Institut Laue-Langevin (Ibel, 1976), using 6.96-Å wavelength neutrons ( $\Delta\lambda/\lambda = 0.08$ ) and a specimen-to-detector distance of 10.5 m. Samples were contained in quartz spectrophotometric cells of 1 or 2 mm path length, which were thermostatically controlled at 25 °C. Data sets were scaled to counts recorded by a beam monitor, and sample transmissions were measured using a semi-transparent beamstop. Data were corrected for detector electronic background and nonlinearity, and were radially averaged in rings subtending  $0.054^\circ$  in scattering angle  $2\theta$ . Buffer backgrounds were subtracted from sample-scattering curves to give radial intensity distributions  $I(Q)$ , where  $Q = 4\pi \sin(\theta)/\lambda$ . Measured sample and corresponding buffer transmissions were within counting statistics of each other in all cases.

## ANALYSIS

The neutron-scattering data was interpreted based on the measurement of two parameters for each sample, the forward scatter  $I(0)$  and the radius of gyration  $R$ , in solvents of different scattering densities. Both quantities

Dr. Gogol's current address is Department of Structural Biology, Stanford University Medical School, Stanford, CA 94306.

were derived by standard Guinier analysis (Guinier and Fournet, 1955) of the very small-angle region of  $I(Q)$ , in each of four or more  $H_2O$ - $D_2O$  mixtures. Linear regions of Guinier plots ( $\ln I(Q)$  vs.  $Q^2$ ) were chosen for analysis, spanning a  $QR$  range of  $\sim 1.0$ – $1.6$  in the case of lipid and cytochrome  $b_5$  vesicles and  $1.0$ – $2.0$  for the trypsinized vesicles. (A constant  $Q$ -region was analyzed for all solvent densities for each type of vesicle.) The forward scatter varies linearly with the solvent-scattering density, as shown in Fig. 1. The point of zero contrast, where the average vesicle-scattering density ( $\rho$ ) equals that of the solvent, is given by extrapolation to zero forward scatter; these values of  $\rho$  are listed in Table I.

The behavior of the radii of gyration of centrosymmetric particles with changes in solvent-scattering density was described by Stuhmann (1974):

$$R^2 = R_c^2 + [\alpha/(\rho - \rho_{soln})], \quad (1)$$

where  $R_c$  is the radius of gyration of the particle at infinite contrast with the solvent, and  $\rho$  and  $\rho_{soln}$  are the scattering density of the particle and solvent. The quantity  $\alpha$  is the second moment of the scattering density distribution in the particle and, for a spherical vesicle, represents the

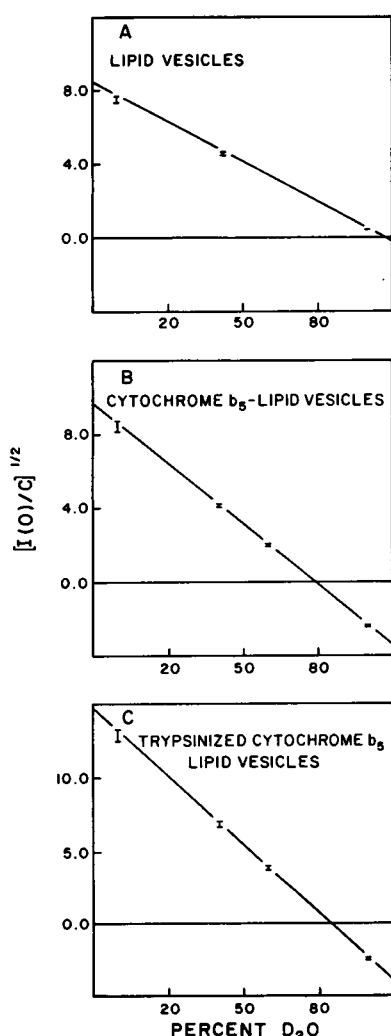


FIGURE 1 Contrast-variation behavior of the square root of forward scatter (normalized to each sample's concentration) is shown for each type of sample. The points of intersection of the linear fits with zero forward intensity give the contrast-match points, the average scattering densities ( $\rho$ ) of the particles.

TABLE I  
EXPERIMENTALLY MEASURED PROPERTIES OF  
THE VESICLE SAMPLES

Sample	$\rho$	$R_c$	$\alpha$
	$10^{-14} \text{ cm}/\text{\AA}^3$	$\text{\AA}$	$10^{-12} \text{ cm}/\text{\AA}$
Lipid vesicles	$6.8 \pm 0.1^*$	$146 \pm 1$	$+7 \pm 1$
Cytochrome $b_5$ vesicles	$4.9 \pm 0.2$	$165 \pm 1$	$-40 \pm 7$
Trypsinized vesicles	$5.3 \pm 0.1$	$238 \pm 2$	$+27 \pm 13$

\*Values are reported with  $\pm$  one standard deviation, calculated by propagation of statistical and experimental errors.

degree of asymmetry across the membrane.  $R_c$  and  $\alpha$  were derived from a plot of  $R^2$  vs. the inverse of the contrast between the particle and the solvent (Stuhmann plot, Fig. 2).  $R_c^2$  is the intercept of the plot with the infinite-contrast axis, and  $\alpha$  is given by its slope; the measured values are listed in Table I.

These quantities are related to more basic physical properties of the vesicles:  $\rho$  is a function of the sample composition,  $R_c$  of the size and shape of the scattering particles, and  $R$  of the arrangement of the vesicle components. To evaluate these properties quantitatively, and to relate them to the structure of cytochrome  $b_5$ , further information must be supplied about the sample. This is done most directly and informatively by constructing low-resolution models of the protein-containing vesicles (based on the different, possible structural arrangements of cytochrome  $b_5$ ), adjusting their parameters to agree with the observed values of  $\rho$  and  $R_c$ , and calculating their second moments. Then, within the overall accuracy of the models, the model that best agrees with the observed value of  $\alpha$  reflects the closest approximation to the actual structure.

Vesicles were modeled as concentric spherical shells of neutron-scattering density. Two shells were used to represent the inner and outer halves of the lipid bilayer. In the case of protein-containing vesicles, a model-dependent fraction of cytochrome  $b_5$  was incorporated into these shells. The total thickness of the bilayer was estimated to be  $44 \text{ \AA}$ , based on multilayer diffraction measurements (Gogol et al., 1983); this dimension was arbitrarily divided between the two shells for modeling purposes. An outer shell was used to represent the extramembranous portion of cytochrome  $b_5$ , together with the water that fills the excess volume of the shell. For calculating the spherically averaged quantities  $R_c$  and  $\alpha$ , this homogeneous shell of averaged protein and solvent-scattering densities is

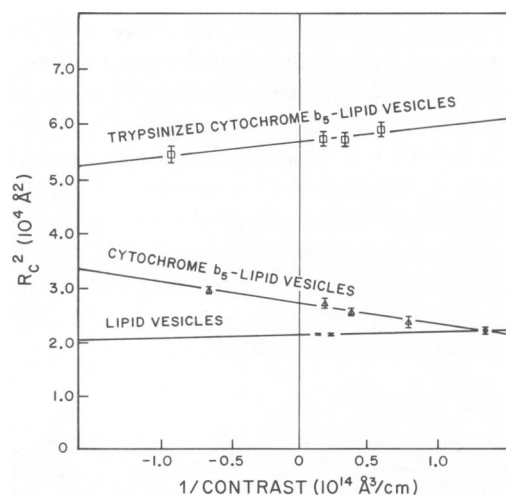


FIGURE 2 Stuhmann plots of the data, together with linear fits, as predicted for particles with a center of symmetry. The slopes of the lines are the values of  $\alpha$ , and their intersections with the zero-value abscissa give values of  $R_c^2$ .

equivalent to a more detailed molecular description. The thickness of this shell was varied to accommodate a range of possible orientations of the catalytic domain from its minimum dimension of 25 Å (Mathews et al., 1970) to 45 Å, which would allow the domain to be tethered to the lipid bilayer by a linking sequence.

The scattering density of each shell was derived from the volume-weighted average of the densities of its components (protein, lipid, and solvent). Lipid-scattering density was obtained from the contrast-match point of the lipid vesicles (Table I), and that of the protein, along with its solvent dependence, was calculated from amino acid molecular volumes and scattering lengths (taken from Jacrot, 1976), assuming 60–80% exchange of labile hydrogens.

The sizes of the vesicles were derived by calculating the physical radii that correspond to the measured values of  $R_c$ . This quantity is dependent on the dimensions of the spherical shells, and not on the arrangement of components, because internal density fluctuations are negligible at infinite contrast. For a single shell of uniform density,  $R_c$  is given by:

$$R_c^2 = \frac{3}{5} \left( \frac{r_o^5 - r_i^5}{r_o^3 - r_i^3} \right), \quad (2)$$

where  $r_o$  and  $r_i$  are the outer and inner radii of the shell. Eq. 2 is valid for particles of uniform size, but for a heterogeneous population of vesicles, the measured value of  $R_c$  is given by a weighted average:

$$R_c^2 = \frac{\sum_i n_i V_i^2 R_{ci}^2}{\sum_i n_i V_i^2}, \quad (3)$$

where  $n_i$  is the fraction of vesicles with volume  $V_i$  and  $R_c$  equal to  $R_{ci}$ . The observed values of  $R_c$  were modeled using Eq. 3, assuming a Gaussian distribution of vesicle sizes about a mean value. The width of the distribution was varied from zero to a value that was sufficiently large to be physically limiting at the low end of the size distribution (a minimum outer radius of at least 100 Å). For the cytochrome  $b_5$  vesicles, this calculation was performed for each of the modeled protein projections from the bilayer because the relationship between the physical radius and  $R_c$  is dependent on the total thickness of the shell.

The second movement of a particle is defined as:

$$\alpha = \frac{1}{V} \int [\rho(r) - \rho] r^2 dV, \quad (4)$$

where  $V$  is the particle volume,  $\rho$  is its average density, and  $\rho(r)$  is its spherically averaged density at radius  $r$ . For a model particle consisting of three concentric spherical shells, this expression is reduced to:

$$\alpha = \frac{\pi}{V} \sum_{n=1}^3 [\rho(n) - \rho] [r_o(n)^5 - r_i(n)^5], \quad (5)$$

where  $\rho(n)$  is the density of the  $n$ th shell, and  $r_o(n)$  and  $r_i(n)$  are the outer and inner radii of the  $n$ th shell. Because of the size heterogeneity of the particles, the observed value of  $\alpha$  is a weighted average, as above:

$$\alpha = \frac{\sum_i n_i V_i^2 \alpha_i}{\sum_i n_i V_i^2}, \quad (6)$$

where  $n_i$  and  $V_i$  are the fraction and volume of particles with a second moment equal to  $\alpha_i$ . Eqs. 5 and 6 were used to calculate values of  $\alpha$  for vesicle models, using the Gaussian size distributions and corresponding radii described above.

Three classes of possible cytochrome  $b_5$  structures, which differed in the arrangements of their hydrophobic domain, were considered in calculating second moments of the vesicles. These three models, schemati-

cally depicted in Fig. 3, are approximations to the actual distribution of the membrane-binding segment, and serve to test the range of reasonable structures. In model A the hydrophobic domain is located outside the bilayer, in the shell occupied by the catalytic domain. In this arrangement very little protein mass interacts with the surface or penetrates the bilayer. Structures in which most of the hydrophobic domain is located in the outer monolayer of the vesicle are represented by model B, in which the scattering density of the tail is evenly distributed in the outer half of the vesicle bilayer. The third model, C, equally partitions the hydrophobic domain between the two halves of the bilayer, representing those possible protein structures that penetrate the bilayer deeply, including those that totally span it. In calculating values of  $\alpha$  for each model of the hydrophobic domain, the projection of the catalytic domain was varied, as was the width of the vesicle size distribution, in order to optimize each model independently.

## RESULTS

Analysis of the scattering properties of the lipid vesicles (Table I) leads to a simple and self-consistent model. The

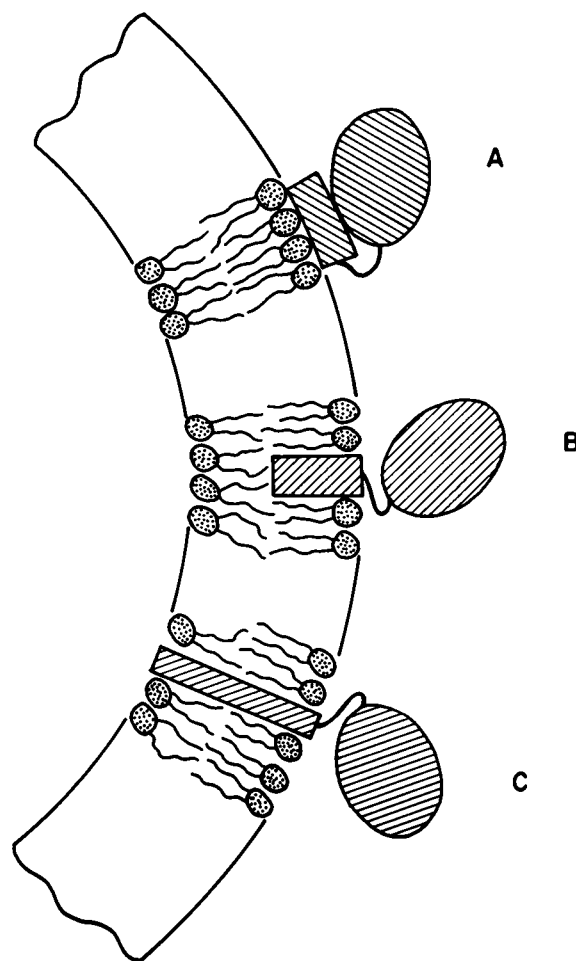


FIGURE 3 The three classes of the cytochrome  $b_5$  hydrophobic domain models that are examined in this study are schematically illustrated. The oval structure represents a cross section of the hydrophilic catalytic domain of the protein, and the rectangle is the modeled distribution of the membrane-binding segment with respect to the lipid bilayer. Several phospholipid molecules have been drawn in approximately to scale. In model A, most of the domain is near the surface of the bilayer; in B, it is distributed in the half of the bilayer proximal to the catalytic domain; and in C, it is evenly distributed in both halves of the bilayer.

measured value of  $\rho$  agrees (within 8%) with the value estimated from atomic scattering lengths, partial molecular volumes, and the lipid composition and deuteration level (~85%). The radii calculated for these vesicles are dependent on their assumed size distribution. For a very narrow Gaussian distribution ( $\sigma \leq 5$  Å), a mean vesicle radius of 165 Å is derived from the observed value of  $R_c$ . Given a wider distribution of sizes, a smaller mean radius is calculated, 148 Å for  $\sigma = 25$  Å. This latter distribution, obtained within the limits  $\pm 2\sigma$ , includes vesicles with radii of only ~100 Å at its lower end, which is probably a physical limit. Therefore, if their distribution can be approximated as Gaussian, the actual mean size of these vesicles is in the range of 165–148 Å. The small positive value of  $\alpha$  observed for these vesicles may result from small differences in lipid-packing density between the two monolayers. Whereas we have not attempted to model this asymmetry in any molecular detail, we have incorporated it into the models of the protein-containing vesicles and found only minor effects on the resulting calculation of  $\alpha$ .

The value of  $\rho$  measured for the cytochrome  $b_5$  vesicles, together with the scattering densities of lipid and protein, have been used to calculate the composition of this sample. The molar lipid-to-protein ratio thus derived is 18.4, which is within experimental error of the value measured spectroscopically, 17.2. To maintain consistency in model building, the value derived from  $\rho$  has been used in further calculations.

Size distributions were modeled for the cytochrome  $b_5$  vesicles as described, using a lipid outer radius of ~100 Å as a lower limit to the size range (at  $2\sigma$  below the mean). This limit was reached for distributions with  $\sigma = 20$ –25 Å, depending on the modeled protein projection for the bilayer. The resulting values of the mean outer radius of the vesicles (including the protein-solvent shell) are listed in Table II. In each case, the radius of the lipid vesicle inside the outer shell is comparable to the range derived above for the lipid vesicles alone.

Using the range of possible protein projections from the bilayer, the second moment of the distribution was calculated for each of the models of the cytochrome  $b_5$  hydrophobic domain. The results are listed in Table II and should be compared with the measured value of  $-40 (\pm 7) \times 10^{-12}$  cm/Å. Somewhat surprisingly, the calculated values of  $\alpha$  are independent of the modeled width of the vesicle size distribution. Whereas neither of the simple models of the membrane-binding segment produced the observed value of  $\alpha$ , it is clear that model C, the most deeply penetrating distribution, gave the best fit. In addition, a compact projection of the catalytic domain from the bilayer surface resulted in the best value of  $\alpha$ .

Analysis of the trypsinized vesicle data is qualified by uncertainties concerning the sample, but leads to the same general conclusion as does the analysis of the native cytochrome  $b_5$  vesicle. Most striking in the scattering data from this sample (Table I) is the reversal of the sign of  $\alpha$ ,

TABLE II  
PARAMETERS DERIVED FROM MODELS OF  
CYTOCHROME  $b_5$  VESICLES

Protein projection from bilayer*	Modeled size range†	Calculated values of $\alpha$		
		model A	model B	model C
	Å	$10^{-12}$ cm/Å		
25	193–178	–97	–82	–58
35	196–180	–113	–92	–70
45	199–188	–130	–103	–82

\*Different models of the distribution of the cytochrome  $b_5$  catalytic domain, as described in the text.

†Outer radii of the model vesicles determined from the measured value of  $R_c$ , assuming a Gaussian size distribution with  $\sigma \leq 25$  Å.

and thus of the average radial relationship of lipid and protein with proteolysis. This effect can be explained only by a model in which 50% or more of the hydrophobic domain is located in the inner half of the lipid bilayer (or, alternatively, inside the vesicle). The apparent size of these vesicles, calculated from the measured value of  $R_c$ , is quite large compared with the previous two samples. Values of ~230–245 Å are derived for the lipid bilayer outer radius (inside the shell containing residual catalytic domains), assuming a narrow size distribution. By allowing a wider size distribution, the mean value of this parameter drops, but insufficiently to match the size measured before trypsin treatment. If this increase in vesicle size is caused by fusion (perhaps induced by the cleaved hydrophobic domain), the nature of the particle may change significantly because of lipid and possibly protein rearrangements. An additional and more serious constraint on the interpretation of these data stems from the contrast-match point calculation, which is consistent with the removal of only 52% of the catalytic domain from the scattering particle, rather than 80% as estimated previously. This discrepancy can be explained only by associating some of the apparently removed protein (minus the heme group) with the vesicles, where protein could possibly be trapped in the contained volume. These considerations make it impossible to model the trypsinized vesicles consistently with all the data.

Nevertheless, barring the possible rearrangement of the vesicles, the only type of cytochrome  $b_5$  structure that can produce a positive value of  $\alpha$  when trypsinized is one whose center of mass is located more than halfway into the bilayer. Within the range of simple models discussed, this is of course represented by model C, which predicts that  $\alpha = 12 \times 10^{-12}$  cm/Å when the catalytic domain is completely removed.

## DISCUSSION

The interpretation of cytochrome  $b_5$  structure presented here rests on the analysis of the very small-angle region of the solution-scattering pattern (Guinier region). In

studying particles of similar size, Jacrot and co-workers (1977) have modeled the extended neutron-scattering curves of RNA viruses. This type of analysis is not possible with the vesicle samples used here because of their size heterogeneity, which smears the subsidiary features of their scattering curves. Hence the analysis depends solely on the small-angle region of the pattern, which inherently has a lower information content than the entire pattern. With additional information about the arrangement of the vesicle components, we have been able to define and constrain the parameters sufficiently to allow us to focus the analysis on differences among three classes of possible cytochrome *b<sub>5</sub>* hydrophobic domain structures. The scattering properties have been calculated for vesicle models that represent each class of the possible protein structures; the differences in their predicted second moments are shown in Table II.

Another facet of size heterogeneity is the interpretation of Guinier plots: an average (size-weighted) rather than single radius of gyration is obtained (Guinier and Fournet, 1955). By analyzing a constant Q-region for each type of vesicle, consistent values of  $I(0)$  and  $R$  were derived that correspond to a constant distribution of sizes; the linearity of the plots in Figs. 1 and 2 confirms this point. In modeling the size heterogeneity, a Gaussian distribution (over  $\pm 2\sigma$ ) has been postulated to approximate the actual variation in vesicle sizes. Varying the width of this distribution over a reasonable range has the effect of altering the modeled mean radius of the vesicles, e.g., decreasing it for wider distributions. The calculated values of  $\alpha$  are surprisingly constant (they vary by  $< \pm 1 \times 10^{-2}$  cm/Å) for any distribution width used.

Compositional homogeneity of the samples has been assumed throughout this analysis. There is no chemically based reason to believe otherwise, and statistical fluctuations are minor because the average size of the vesicles is  $\sim 1,900$  lipid and  $\sim 110$  protein molecules. Total asymmetry of the native cytochrome *b<sub>5</sub>* vesicles was determined as previously described (Gogol et al., 1983). A generous error limit on this measurement is 5%; incorporation of this degree of symmetry does not affect the relative merit of the protein models. In fact, this amount of partial symmetry brings the values of  $\alpha$  calculated for model C closer to the observed value.

Particular features of the molecular arrangement of cytochrome *b<sub>5</sub>* are strongly favored by our analysis. In the context of the models considered for possible protein structures, the hydrophobic domain is best represented by model C. In addition, the disposition of the catalytic domain in these vesicles seems to be fairly close to the bilayer, as indicated by the variation of models for the protein projection (Table II). Both of these features agree with an independent treatment of lamellar neutron diffraction data collected from cytochrome *b<sub>5</sub>*-lipid multilayers (Gogol et al., 1983). It is unfortunate that the analysis of the trypsinized vesicles is hindered by ambiguities about

the sample; the only conclusion that may safely be reached about that data is that it is most consistent with model C.

The essential feature of the favored structural arrangement of the hydrophobic domain is that it is located deep in the lipid bilayer, with portions in both halves of the membrane. This arrangement does not necessarily imply that the protein crosses the bilayer entirely, although membrane-spanning structures are of course entirely consistent with this model. Alternative protein arrangements that place the center of mass far into the bilayer are conceptually possible. However, other types of suggested structures, for example those that place all of the hydrophobic domain only in one half of the bilayer, are excluded by these results.

We are grateful to Dr. G. Zaccai for his help in data collection and interpretation, and to Dr. Philipp Strittmatter for providing the protein used in this work, along with helpful advice. We thank the Institut Laue Langevin for use of their facilities, and Dr. J. M. Freyssinet and the European Molecular Biology Laboratory for providing facilities for some of the sample preparation.

This work was supported by grants from the National Institutes of Health (GM22778) and the National Science Foundation (PCM78-10361).

Received for publication 2 March 1983 and in final form 30 March 1984.

## REFERENCES

- Barlett, G. R. 1959. Phosphorous assay in column chromatography. *J. Biol. Chem.* 234:466-468.
- Dailey, H. A., and P. Strittmatter. 1981. Orientation of the carboxy and NH<sub>2</sub> termini of the membrane-binding segment of cytochrome *b<sub>5</sub>* on the same side of phospholipid bilayers. *J. Biol. Chem.* 256:3951-3955.
- Fleming, P. J., D. E. Koppel, A. L. Y. Lau, and P. Strittmatter. 1979. Intramembrane position of the fluorescent tryptophanyl residue in membrane-bound cytochrome *b<sub>5</sub>*. *Biochemistry*. 18:5458-5464.
- Gogol, E. P., G. Zaccai, and D. M. Engelman. 1983. Neutron diffraction analysis of cytochrome *b<sub>5</sub>* reconstituted in deuterated lipid multilayers. *Biophys. J.* 43:285-292.
- Guinier, A., and G. Fournet. 1955. Small-Angle Scattering of X-rays. John Wiley and Sons, Inc. NY.
- Ibel, K. 1976. The neutron small-angle camera D11 at the high-flux reactor, Grenoble. *J. Appl. Crystallogr.* 9:296-309.
- Jacrot, B. 1976. The study of biological structures by neutron scattering from solution. *Rep. Progr. Phys.* 39:911-953.
- Jacrot, B., C. Chauvin, and J. Witz. 1977. Comparative neutron small-angle scattering study of small spherical RNA viruses. *Nature (Lond.)*. 266:417-421.
- Mathews, F. S., P. Argos, and M. Levine. 1970. Comparative neutron small-angle scattering study of small spherical RNA viruses. *Nature (Lond.)*. 266:417.
- Osborne, H. B., C. Sardet, M. Mdichel-Villaz, and M. Chabre. 1978. Structural study of rhodopsin in detergent micelles by small-angle neutron scattering. *J. Mol. Biol.* 123:177-206.
- Spatz, L., and P. Strittmatter. 1971. A form of cytochrome *b<sub>5</sub>* that contains an additional hydrophobic sequence of 40 amino acid residues. *Proc. Natl. Acad. Sci. USA* 68:1042-1046.
- Strittmatter, P., P. J. Fleming, M. Connors, and D. Corcoran. 1978. Purification of cytochrome *b<sub>5</sub>*. *Methods Enzymol.* 52:97-101.
- Stuhrmann, H. B. 1974. Neutron small-angle scattering of biological macromolecules in solution. *J. Appl. Crystallogr.* 7:173.
- Yeager, M. J. 1975. Neutron diffraction analysis of the structure retinal photoreceptor membranes and rhodopsin. *Brookhaven Symp. Biol.* 27:111-3.